# Copolymer–homopolymer mixtures in a nanopore*

Zhang Ling-Cui(张玲翠), Sun Min-Na(孙敏娜) Pan Jun-Xing(潘俊星), Wang Bao-Feng(王宝凤), Zhang Jin-Jun(张进军)†, and Wu Hai-Shun(武海顺)

*School of Chemistry and Materials Science, Shanxi Normal University, Linfen* 041004, *China*

(Received 18 December 2012; revised manuscript received 5 March 2013)

We have performed the cell dynamics simulation with the time-dependent Ginzburg–Landau theory to study the self-assembled morphology of A–B diblock copolymers and C homopolymers in a neutral nanopore. The nanopore diameter and length are systematically varied to examine their effects on the structures of various morphologies and their phase transition. From the simulation, it is observed that the equilibrium morphology of the confined system is sensitive to pore diameter $D$ and pore length $L_{\rm pore}$, the phase behavior in neutral nanopores is due to an interplay of two factors: the surface effect and the extension effect. When the nanopore length and the lamellae spacing are not commensurate, the surface effect prevails at small nanopores (small diameters or short lengths), the extension effect takes over at larger nanopores (large diameters or long lengths). When the nanopore length and the lamellae spacing are commensurate, the surface effect dominates. Furthermore, the interactions between different monomers are also discussed and we obtain a transition from a tilted pancakes/cylinder structure ($L_{\perp}^{\rm tilted}$) to a concentric cylindrical structure with defects and to a concentric cylindrical structure ($L_{\parallel}$). We also investigate the effect of the relative concentrations of diblock copolymer–homopolymer and obtain a transition in which the position of the C blocks changes from the outer of the cylinder to the middle of the cylinder and then to the inner of the cylinder with the concentration of the C blocks decreasing.

**Keywords:** copolymer–homopolymer mixtures, nanopore, self-assembled morphology, phase transition

**PACS:** 64.75.Va, 64.75.Yz, 83.80.Uv, 83.80.Tc **DOI:** 10.1088/1674-1056/22/9/096401

## 1. Introduction

The phase behavior of block copolymer melts has been the focus of a substantial amount of theoretical and experimental investigations due to the interesting applications in nanotechnology and biological areas.[1–7] Applying external fields is a promising method to obtain a desired nanostructure. Such fields can be surface fields,[8–14] electric fields,[15–20] and shear flows.[21–23] The surface fields are, in particular, prominent in confined geometries. Confinement is a powerful tool to break the symmetry of a structure, allowing materials to self-assemble into new morphologies that usually are not present in the bulk. Therefore, the phase behavior of the polymer system under a cylindrical nanopore confinement has a variety of potential applications. According to the confined geometries, confinement can be divided into three kinds: one-dimensional (1D) confinement,[24–32] two-dimensional (2D) confinement,[33–67] and three-dimensional (3D) confinement.[68–80]

So far, the research on the 1D confinement has reached a mature stage, and the 2D confinement of block copolymers has attracted more attention. The phase behavior of confined systems have been studied in theory by means of the self-consistent field theory (SCFT), Monte–Carlo (MC) simulations, dissipative particle dynamics (DPD) methods, molecular dynamics simulation (MD) methods, and cell dynamics simulation (CDS) methods. Using MC calculations, Chen *et al.*[49] observed a variety of morphologies, including stacked-disk, single-helix, catenoid-cylinder, gyroidal, stacked-circle, and concentric cylindrical barrel structures. Feng *et al.*[52] observed the lamellae normal to the tube axis, circular lamellae, mesh, lamellae parallel to the pore axis, single helix, and double-helix structures. Using the DPD simulation, Feng *et al.*[51] found double helices, stacked disks, and parallel lamellae. Wu *et al.*[45] used the SCFT calculations to predict the behavior of a cylinder-forming system in cylindrical nanopores. They found that with the increasing diameter, spheres, straight cylinders, helix, multihelix, and finally the concentric inner shells form. Their results are in a good agreement with the experimental results. Yu *et al.*[62,63] studied a cylinder-forming asymmetric diblock copolymer confined in cylindrical pores using the simulated annealing technique. They found many novel structures that were not present in the bulk ranging from spheres and cylinders to helices and toroids. Using the MD simulation, Li *et al.*[67] found that a graphene nanoribbon (GNR) could helically wrap and be inserted into a single-walled carbon nanotube (SWNT) to form helical configurations. Using the CDS simulation, Pinna *et al.*[57] studied in detail the lamellar-, cylinder-, and eventu-

*Project supported by the National Natural Science Foundation of China (Grant No. 21031003), the Natural Science Foundation of Shanxi Province, China (Grant No. 2007011055), the Soft Science Program of Shanxi Province, China (Grant No. 2011041015-01), the Specialized Research Fund for the Doctoral Program of Higher Education of China (Grant Nos. 20121404110004 and 20091404120002), and the Research Foundation for Excellent Talents of Shanxi Provincial Department of Human Resources and Social Security, China.

†Corresponding author. E-mail: zhangjinjun@sxnu.edu.cn

© 2013 Chinese Physical Society and IOP Publishing Ltd 

ally sphere-forming diblock copolymer melts in cylindrical nanopores. The structures they observed were controlled by the interplay of four factors: pore diameter, affinity of the pore wall to the copolymer blocks, block copolymer composition, and the mismatch between the pore length and the domain spacing, which led to the formation of many novel structures that were not present in the bulk block copolymer systems. Most of the above mentioned studies have focused on the self-assembly of individual block copolymers. It is significant to study the self-assembly of complex polymers under confinement. The self-assembly of mixtures of block copolymers and homopolymers in a solution has also been studied.[81–85] One of the authors, Zhang, and coworkers, studied the phase separations of a copolymer–homopolymer mixture under oscillatory particles and observed the orientational order transition of a striped microphase structure from the isotropic state to a state parallel to the oscillatory direction, and from the parallel state to a state perpendicular to the oscillatory direction,[81] then they studied the phase separation of a copolymer–homopolymer mixture containing doping wettable nanoparticles with a preferential attraction for one component of the copolymers and obtained many novel structures, such as single stripes, hexagonal chains, and bistripes in microphase stripe structure.[82] Later, they studied the phase separation in a diblock copolymer–diblock copolymer mixture and obtained an onion-ring morphology.[83] Therefore, we choose the cell dynamics simulation method to systematically investigate the self-assembly of mixtures of copolymer–homopolymer under a cylindrical confinement, and we find many novel self-assembled structures which may aid in the design of novel polymeric nanomaterials under confinement.

This paper is organized as follows. In Section 2, we describe the model and the CDS method. In Section 3, we discuss the effects of pore confinement and repulsive interactions between different monomers on the phase separation as well as the effect of the relative concentrations of A–B diblock copolymers and C homopolymers. In the last section, we provide a short summary.

## 2. Model and method

We consider a system which consists of A–B diblock copolymers and C homopolymers in a cylindrical pore. Each copolymer chain is composed of monomers A and B with a short-range repulsive interaction between them. The interaction between monomer C in a homopolymer and monomer B in a copolymer is also assumed to be repulsive. In addition, the hydrodynamic effects, which prevail in the very latest stage of phase separation in polymer blends, are neglected in the present model. We use $\chi_{ijk}$ to denote the interaction between monomers $i$, $j$, and $k$, where $i$, $j$, $k$ = A, B, C. In the process of phase separation, fluctuations are dominant, so we should investigate the local volume fractions of monomers A, B, and C. They are denoted, respectively, by $\phi_{\rm A}(x,y,z)$, $\phi_{\rm B}(x,y,z)$, and $\phi_{\rm C}(x,y,z)$. The polymerization indices of these polymers are $N_{\rm A}$, $N_{\rm B}$, and $N_{\rm C}$, respectively. The block ratio of a block copolymer, $f$, is defined as $f = N_{\rm A}/(N_{\rm A}+N_{\rm B})$. In this paper, we restrict ourselves to diblock copolymers with $f = 1/2$ (or $N_{\rm A} = N_{\rm B}$) in order to understand the essence of the phase separation phenomena in A–B/C systems. Under the incompressibility condition, two of the local volume fractions are independent. It is convenient to take $\varphi(x,y,z) = \phi_{\rm A}(x,y,z) + \phi_{\rm B}(x,y,z)$ and $\phi(x,y,z) = \phi_{\rm A}(x,y,z) - \phi_{\rm B}(x,y,z)$ as the independent variables. The variable $\varphi(x,y,z)$ is useful to describe the segregation of copolymers and homopolymers, while $\phi(x,y,z)$ plays the role of an order parameter in the microphase separation. Furthermore, we use $\eta(x,y,z) = \varphi(x,y,z) - \varphi_{\rm c}$ instead of $\varphi(x,y,z)$, where $\varphi_{\rm c}$ is the volume fraction at the critical point of the macrophase separation and is a constant determined by the paremeters of the system.

Here we propose a two-order-parameter model.[86–89] The free energy of the system is given by

$$F = F_{\rm L} + F_{\rm S}. \tag{1}$$

The long-range part $F_{\rm L}$ and the short-range part $F_{\rm S}$ are given by

$$F_{\rm L} = \frac{\alpha}{2}\iint {\rm d}\boldsymbol{r}\,{\rm d}\boldsymbol{r}' G(\boldsymbol{r},\boldsymbol{r}')[\phi(\boldsymbol{r})-\phi_0][\phi(\boldsymbol{r}')-\phi_0], \tag{2}$$

$$F_{\rm S} = \iiint {\rm d}\boldsymbol{r}\Big[\frac{D_1}{2}(\nabla\eta(\boldsymbol{r}))^2 + \frac{D_2}{2}(\nabla\phi(\boldsymbol{r}))^2 + f_\eta(\eta) + f_\phi(\phi) + f_{\rm int}(\eta,\phi)\Big], \tag{3}$$

where $\alpha$, $D_1$, and $D_2$ are all positive constants. The long-range part is relatively simple, in which $G(\boldsymbol{r},\boldsymbol{r}')$ is the Green's function defined by the equation $-\nabla^2 G(\boldsymbol{r},\boldsymbol{r}') = \delta(\boldsymbol{r}-\boldsymbol{r}')$, and $\phi_0$ is the spatial average of $\phi$. We must set $\phi_0 = 0$ in the case of symmetric copolymers. As for the short-range part, the $D_1$ and $D_2$ terms correspond to the surface tensions. Functions $f_\eta$ and $f_\phi$ are assumed to be even functions and have double minima below the respective critical temperatures. We choose the following interaction between $\eta$ and $\phi$:

$$f_{\rm int}(\eta,\phi) = b_1\eta\phi - \frac{b_2}{2}\eta\phi^2. \tag{4}$$

Equation (4) describes the minimal model of the short-range part of the free energy in our system. In the symmetric case, $b_1 = (-\chi_{\rm AC}+\chi_{\rm BC})/2$, $b_2 = 1/(\varphi_{\rm c}^2 N_{\rm A})$. It is now clear that the $b_1$ term mainly originates from the interaction between the A–B copolymer and the C monomer. If the repulsive interaction strength $\chi_{\rm BC}$ between B and C is large enough, $b_1$ is positive. The $b_2$ term represents the fact that the microphase separation should occur only in the copolymer-rich phase. In terms of the free energy in Eqs. (1)–(4), we obtain a set of two coupled

equations

$$\frac{\partial \eta}{\partial t} = M_\eta \nabla^2 \frac{\delta F}{\delta \eta}, \quad (5)$$

$$\frac{\partial \phi}{\partial t} = M_\phi \nabla^2 \frac{\delta F}{\delta \phi}, \quad (6)$$

where $M_\eta$ and $M_\phi$ are the transport coefficients, the relative magnitude of these two coefficients is not known experimentally, so we set $M_\eta = M_\phi = 1.0$ for simplicity.

We carry out computer simulations of the model system in three dimensions by using the cell dynamical simulation proposed by Oono and Puri,[90–92] and the CDS equations corresponding to Eqs. (5) and (6) in their space–time discretized forms are written as

$$\eta(x,y,z,t+\Delta t) = \eta(x,y,z,t) + M_\eta(\langle\langle I_\eta\rangle\rangle - I_\eta), \quad (7)$$

$$\phi(x,y,z,t+\Delta t) = \phi(x,y,z,t) + M_\phi\{(\langle\langle I_\phi\rangle\rangle - I_\phi) - \alpha[\phi(x,y,z,t) - \phi_0]\}, \quad (8)$$

where

$$I_\eta = -D_1(\langle\langle\eta\rangle\rangle - \eta) - A_\eta \tanh\eta + \eta + b_1\phi - \frac{1}{2}b_2\phi^2, \quad (9)$$

$$I_\phi = -D_2(\langle\langle\phi\rangle\rangle - \phi) - A_\phi \tanh\phi + \phi + b_1\eta - b_2\eta\phi, \quad (10)$$

$$\langle\langle X\rangle\rangle = \frac{6}{80}\sum_{\mathrm{NN}} X + \frac{3}{80}\sum_{\mathrm{NNN}} X + \frac{1}{80}\sum_{\mathrm{NNNN}} X. \quad (11)$$

Here subscripts NN, NNN, and NNNN stand for nearest-neighbor, next-nearest-neighbor, and next-next-nearest-neighbor cells, respectively.

In our simulations, we set $M_\eta = M_\phi = 1$, $D_1 = 1.0$, $D_2 = 0.5$, $\phi_0 = 0.0$, $b_2 = 0.2$, $A_\eta = 1.1$, $A_\phi = 1.12$. According to the previous work, in the present simulation, in the case of $\alpha = 0.02$, by the formula $\alpha = 12/N^2 f_\mathrm{b}(1-f_\mathrm{b})$ ($f_\mathrm{b}$ denotes a block ratio), we can obtain $N_\mathrm{A} = N_\mathrm{B} = 24$, $N_\mathrm{C} = 34$, $\chi_{\mathrm{AB}}N_{\mathrm{AB}} = 20.26$.

## 3. Numerical results and discussion

### 3.1. Lamellae period $L_0$ in bulk states

Equilibrium bulk phases are obtained in rectangular boxes of sizes $L_x \times L_y \times L_z$ with the periodic boundary conditions in all three directions. The composition ratio of C to A–B is 59.4/40.6, $b_1 = 0.001$, and $L_x$, $L_y$, and $L_z$ are varied so that the box is commensurate to the period of the ordered structure. In order to probe the lamellae period $L_0$ of A–B diblock copolymers in the mixture, we obtain the morphological patterns in a $20 \times 20 \times 20$ lattice, as shown in Fig. 1. The black, pink, and green regions stand for A-rich, B-rich, and C-rich regions, respectively. For clearness, we denote the A-rich domain for $\phi > 0$ and the B-rich domain for $\phi < 0$, whereas the C-rich domain for $\eta < 0$.

From Fig. 1, we can see A–B diblock copolymers form four lamellae periods with a sequence of A–B–A–B–A–B–A–B, and blocks C aggregate to the surface which is perpendicular to the A–B diblock. In the case of $b_1 = 0.001$, we can figure out $\chi_{\mathrm{AC}} = 0.227$ and $\chi_{\mathrm{BC}} = 0.229$. We can see that the repulsive interactions between the A, B blocks and the homopolymer are nearly equal ($\chi_{\mathrm{AC}} \approx \chi_{\mathrm{BC}}$), which means that phases A and B have the same chance to get in touch with phase C. In our simulations, the distance between blocks A and B is varied, so we can choose the distance between blocks A and B ($L_0 = 7.1$) to be compared with the size of the nanopore. In addition, we also investigate the lamellae period ($L$) of A–B diblock copolymers and C homopolymers in the bulk states, and we observe a series of concentric cylindrical structures with the pore diameter $D$ and pore length $L_{\mathrm{pore}}$ increased.

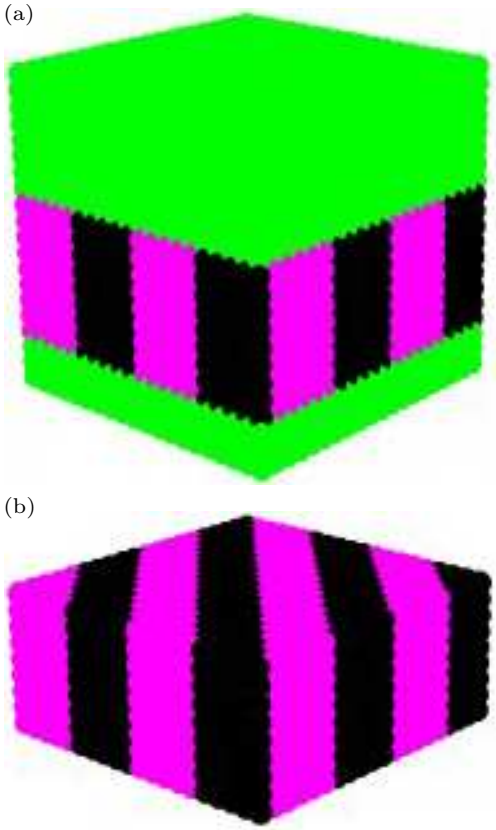



**Fig. 1.** (color online) Morphological pattern in a $20 \times 20 \times 20$ lattice with the composition ratio of C to A–B being 59.4/40.6, $b_1 = 0.001$: (a) three-dimensional structure, (b) copolymers structure. Phase A is represented by the black regions, phase B by the pink regions, and phase C by the green regions.

### 3.2. Effects of nanopore diameter

For the simulations of confined self-assembly, the A–B diblock copolymers and C homopolymers are confined in a long cylindrical nanopore of diameter $D$. The confinement is realized in the volume $V = L_x \times L_y \times L_z$ with $L_x = L_y = D + m$ and $L_{\mathrm{pore}} = L_z$, where $m = 2$ when $D$ is odd and $m = 3$ when $D$ is even. Polymers cannot occupy the wall sites which are the lattice sites outside the cylinder with diameter $D$. Therefore the polymers are confined in an approximate cylindrical nanopore of diameter $D$.[50] The extra $m$ in $L_x$ and $L_y$ ensures that each site inside the cylindrical nanopore has 26 neighbor sites. These neighbor sites are either inside the pore or in the wall. We choose the most simple model, in which the

preference of copolymer blocks to surfaces is described by the Dirichlet boundary condition.[57]

In our simulations, we use the neutral surface with various nanopore diameter, the composition ratio of C to A–B is 59.4/40.6, $b_1 = 0.001$, and $L_{\rm pore}/L_0 = 5.3$. Figure 2 displays the structures of diblock copolymers and homopolymers mixtures within cylinders of various diameters, we find a more complex situation ranging from piled pancakes/cylinder structure, tilted pancakes/cylinder structure, and multiple helices/cylinder structure. These structures for symmetric diblock copolymers and homopolymers mixtures in a neutral cylindrical nanopore are not found. When $D/L_0 = 5.1$ (Fig. 2(a)), diblock copolymers A–B form a piled-pancake structure in the center of the cylinder, whereas homopolymers C form an outer cylindrical layer, and blocks A and B form piled-pancake structures. Moreover, these A and B disks are aligned perpendicular to the cylinder axis ($L_\perp$). However, above a certain diameter, this structure is not found (Fig. 2). When $D/L_0 = 5.7$–$5.9$ and $D/L_0 = 6.5$–$6.9$ (Figs. 2(b) and 2(d)), diblock copolymers A–B form a double-helix structure in the center of the cylinder, homopolymers C form an outer cylindrical layer, blocks A and B form single-helix structures. When $D/L_0 = 6.1$–$6.3$ and $D/L_0 = 7.3$ (Figs. 2(c) and 2(e)), diblock copolymers A–B form a tilted-pancake structure ($L_\perp^{\rm tilted}$) in the center of the cylinder, homopolymers C form an outer cylindrical layer, and blocks A and B form tilted-pancake structures. When $D/L_0 = 7.6$ (Fig. 2(f)), diblock copolymers form a quadrupole-helix structure in the center of the cylinder, homopolymers C form an outer cylindrical layer, blocks A and B form double-helix structures. In addition, we find that the final morphology of the orther system in a nanopore can also form helical structures. Li *et al.*[65] studied the interaction between a graphene nanoribbon and a single-wall carbon nanotube (SWCNT), they observed that the GNR can enter the SWCNT and form a helical configuration spontaneously.

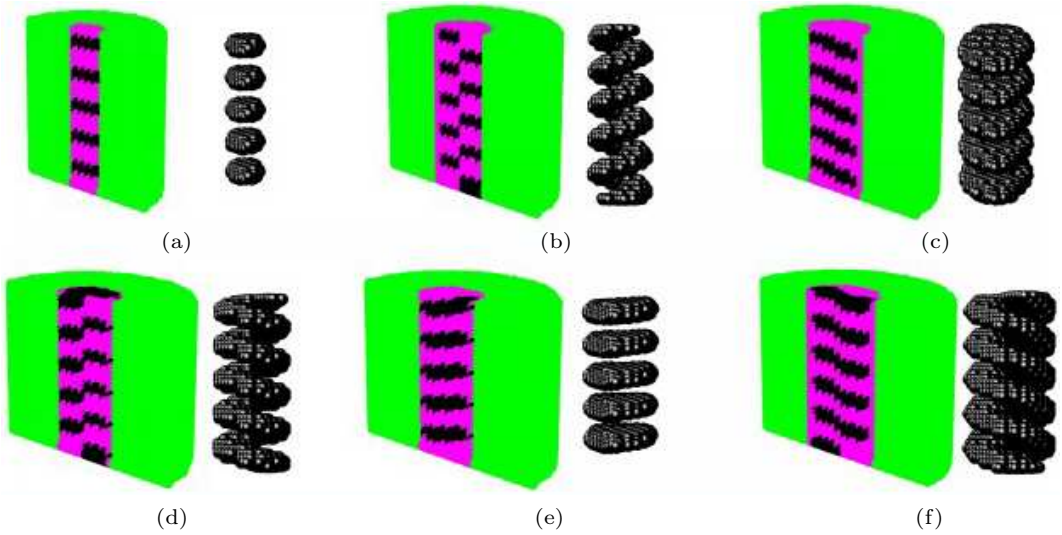



**Fig. 2.** (color online) Morphological patterns constrained in cylinders of various diameters with the composition ratio of C to A–B being 59.4/40.6, $b_1 = 0.001$, $L_{\rm pore}/L_0 = 5.3$, (a) $D/L_0 = 5.1$; (b) $D/L_0 = 5.7$–$5.9$; (c) $D/L_0 = 6.1$–$6.3$; (d) $D/L_0 = 6.5$–$6.9$; (e) $D/L_0 = 7.3$; (f) $D/L_0 = 7.6$. The left of each graph shows the section structure, the right of each graph shows block A. Phase A is represented by the black regions, phase B by the pink regions. Phase C by the green regions.

It is interesting to notice that the structures shown in Fig. 2 exhibit periodicity along the pore. The pitch of these helices or two neighboring lamellae is slightly larger than the equilibrium spacing between the layers in the bulk phase ($L_0$). We observe a piled pancakes/cylinder morphology in the nanopore of a small diameter ($D/L_0 = 5.1$). When the nanopore diameter increases, it is interesting to notice that helices/cylinder and tilted pancakes/cylinder morphologies are repeated alternately in the radial direction. When $L_{\rm pore}/L_0$ is slightly smaller than $nL_0$, helices/cylinder morphologies appear ($D/L_0 = 5.7$–$5.9$, $6.5$–$6.9$, $7.6$); when $L_{\rm pore}/L_0$ is slightly larger than $nL_0$, tilted pancakes/cylinder morphologies appear ($D/L_0 = 6.1$–$6.3$, $7.3$). It is worth mentioning that a similar conclusion has been obtained by Pinna *et al.*[57] already. They discovered that for the diblock copolymer in a neutral nanopore of $D/L_0 \geq 2.24$, the helical and tilted pancakes morphologies are alternately repeated.

For the above mentioned phenomenon, we have the following explanations. The phase behavior in neutral nanopores is due to the interplay of two factors: the surface effect produced by the confinement boundary and the extension effect when the nanopore length and the lamellae spacing are not commensurate. For $D/L_0 \leq 5.1$ (Fig. 2(a)), the surface effect is strong, the elastic chain deformation associated with the parallel structures is avoided, and the perpendicular structures are favored instead. Due to the strong surface effect, the parallel structures (surface reconstructions) will be promoted by surface fields above a certain threshold field strength. The effect

of the neutral surface, which prefers $L_{\perp}$, scales with the surface area up to large surface field strengths. For $D/L_0 > 5.7$, the surface effect has a limited range, the extension effect takes over. We know that the available space in the confined geometry dictates the degree of chain compression or extension. When the diameter of the nanopore increases, the available space also increases, which requires for parallel structures, but the extension effect prevents the parallel structures, the novel helices/cylinder and tilted pancakes/cylinder structures are formed instead. When a tilted pancakes/cylinder structure transforms into a helical/cylinder structure, the reconnection of the domains in the tilted pancake/cylinder structure should take place. Such a reconnection of the domains requires a large amount of deformation energy when the diameter of the cylinder is large. Therefore, the helical/cylinder domains are observed only for the case with a smaller diameter of the cylindrical domain (Fig. 2(b)), and the tilted pancake/cylinder structures for the larger diameter of the cylindrical domain (Fig. 2(c)). Moreover, as the nanopore diameter continues to increase, the available space increases, large chain frustrations give rise to an entropically unfavorable situation and may even prevent the formation of tilted pancakes/cylinder structures, alternative structures are then formed instead (Figs. 2(d)–2(f)). For the above result, we also investigate the case in which the nanopore length and the lamellae spacing are commensurate.

Figure 3 displays the structures of diblock copolymers and homopolymers mixtures in cylinders of various diameters, the composition ratio of C to A–B is 59.4/40.6, $L_{\text{pore}}/L_0 = 4.0$, $b_1 = 0.001$. Figure 3 shows piled pancakes/cylinder structures in the nanopore of the same diameters ($D/L_0 = 5.7$, 6.2–6.3, 6.6), where the helices/cylinder and tilted pancakes/cylinder structures are present in Fig. 2. An interesting observation is that the piled pancakes/cylinder structures always form with changing nanopore diameter (Fig. 3). When the nanopore length and the lamellae spacing are commensurate, the final morphology is independent of the nanopore diameter, the distance between two neighboring lamellae has the same value as $L_0$. When the nanopore length and the lamellae spacing are commensurate, the extension effect has little effect, the surface effect takes over, and the piled pancakes/cylinder structures are formed. Our results are in good agreement with the results of Yu *et al.*,[62] who studied the diblock copolymer in a neutral nanopore.

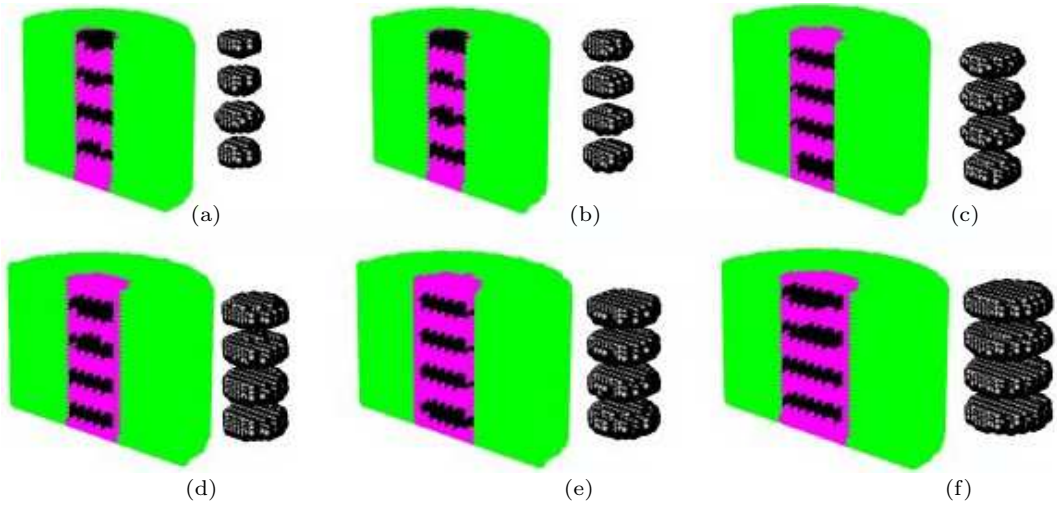



**Fig. 3.** (color online) Morphological patterns constrained in cylinders of various diameters with the composition ratio of C to A–B being 59.4/40.6, $b_1 = 0.001$, $L_{\text{pore}}/L_0 = 4.0$, (a) $D/L_0 = 5.0$; (b) $D/L_0 = 5.1$–5.4; (c) $D/L_0 = 5.6$–5.7; (d) $D/L_0 = 6.0$; (e) $D/L_0 = 6.2$–6.3; (f) $D/L_0 = 6.6$. The left of each graph shows the section structure, the right of each graph shows blocks A. Phase A is represented by the black regions, phase B by the pink regions, phase C by the green regions..

### 3.3. Effects of nanopore length

From the previous work of the cylindrically confined system, it is found that the length of the nanopore as well as the diameter plays an important role. In order to study the effect of the different nanopore length on the morphology, we regulate the nanopore diameter ($D/L_0 = 7.3$), the other parameters are the same as those in Fig. 2. Similar to the bulk phases, the nanopore length $L_{\text{pore}}$ is varied to obtain optimal equilibrium ordered structures. Figure 4 shows the evolution patterns of the mixture with different pore lengths, when similar structures are found for a range of $L_{\text{pore}}/L_0$ (indicated by a hyphen), only representative examples are shown. For $L_{\text{pore}}/L_0 = 4.0$, 5.0 (Figs. 4(a) and 4(d)), diblock copolymers A–B form a piled-pancake structure in the center of the cylinder, whereas homopolymers C form an outer cylindrical layer, and blocks A and B form piled-pancake structures. For $L_{\text{pore}}/L_0 = 4.2$–4.4, 5.1–5.4 (Figs. 4(b) and 4(e)), diblock copolymers A–B form a double-helix structure in the center of the cylinder, homopolymers C form an outer cylindrical layer, blocks A and B form single-helix structures. For $L_{\text{pore}}/L_0 = 4.5$–4.6, 5.5–5.8

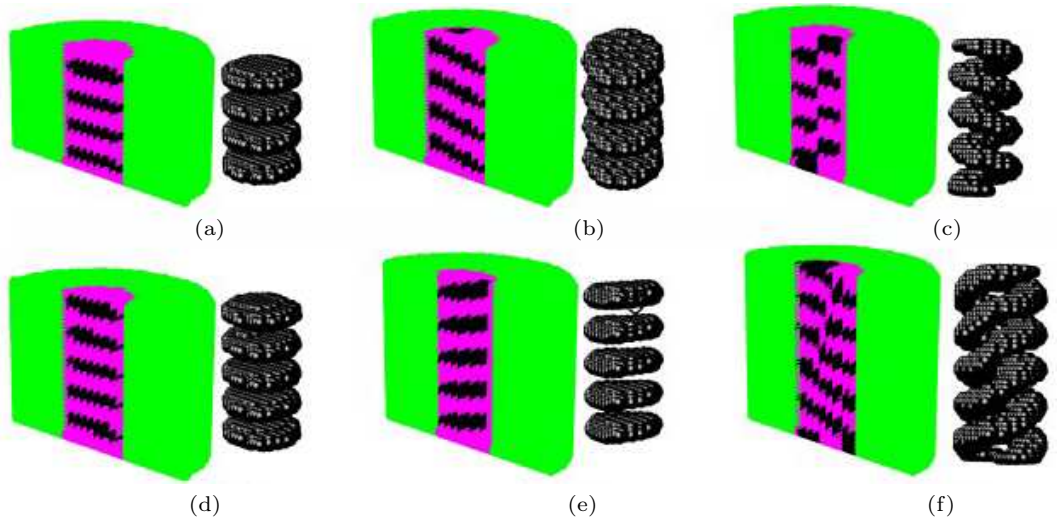



**Fig. 4.** (color online) Morphological patterns constrained within cylinders of various $L_{\rm pore}/L_0$ with the composition ratio of C to A–B being 59.4/40.6, $D/L_0 = 7.3$, other parameters are the same as those in Fig. 2: (a) $L_{\rm pore}/L_0 = 4.0$, (b) $L_{\rm pore}/L_0 = 4.2$–$4.4$, (c) $L_{\rm pore}/L_0 = 4.5$–$4.6$, (d) $L_{\rm pore}/L_0 = 5.0$, (e) $L_{\rm pore}/L_0 = 5.1$–$5.4$, (f) $L_{\rm pore}/L_0 = 5.5$–$5.8$. When similar structures are found for a range of $L_{\rm pore}/L_0$ (indicated by a hyphen), only representative examples are shown, the left of each graph shows the section structure, the right of each graph shows blocks A. Phase A is represented by the black regions, phase B by the pink regions, phase C by the green regions.

(Figs. 4(c) and 4(f)), diblock copolymers A–B form a tilted-pancake structure in the center of the cylinder, homopolymers C form an outer cylindrical layer, blocks A and B form tilted-pancake structures.

We notice that the structures shown in Fig. 4 exhibit periodicity along the nanopore. The pitches of these helices or two neighboring lamellae have different values with varied nanopore length. The structures shown in Fig. 4 also exhibit a repeating pattern in the radial direction, which is different from that in Fig. 2. Furthermore, the simulation results show that when $L_{\rm pore}/L_0$ is close to an integer (Figs. 4(a) and 4(d)), the final morphology is the piled pancakes/cylinder structure, the distance between two neighboring lamellae equals to $L_0$. When $L_{\rm pore}/L_0$ is not an integer (Figs. 4(b), 4(c), 4(e), and 4(f)), the final morphology is the helices/cylinder or tilted pancakes/cylinder structure, the pitch of these helices or two neighboring lamellae is slightly larger than $L_0$.

For the above phenomenon, we can give the following explanation. On one hand, when $L_{\rm pore}/L_0$ is close to an integer, the surface effect is strong, the final morphology is independent of $L_{\rm pore}$. The free energy minimization drives the final morphology to be the lamellae structure perpendicular to the axis of the nanopore (Figs. 4(a) and 4(d)). On the other hand, when $L_{\rm pore}/L_0$ is not an integer, the extension effect takes over, the final morphology is slightly dependent on $L_{\rm pore}$, the tilted pancakes/cylider and helical/cylinder structures are formed (Figs. 4(b), 4(c), 4(e), and 4(f) ), the mechanism of the conversion between helical and tilted morphologies is analogous to that given in the previous section. As the nanopore length continues to increase, the confinement increases, the extension effect diminishes relatively, we predict that the final morphology is the piled pancakes/cylider structure, which needs to be further studied. As a result, when the nanopore length and the lamellae spacing are not commensurate, the extension effect prevails at short lengths, the surface effect takes over at long lengths; when the nanopore length and the lamellae spacing are commensurate, the surface effect dominates.

### 3.4. Effect of the interactions between different monomers

In this section, we discuss the value of $b_1$ for the repulsive interaction between the B block and a homopolymer. Figure 5 displays the domain pattern at $t = 1000000$ with the variation of parameter $b_1$ from 0.001, 0.035 to 0.1, $L_{\rm pore}/L_0 = 5.63$, the other parameters are the same as those in Fig. 4. For $b_1 = 0.001$ (Fig. 5(a)), diblock copolymers A–B form a tilted-pancake structure in the center of the cylinder, whereas homopolymers C form an outer cylindrical layer, blocks A and B form tilted-pancake structures. For $b_1 = 0.035$ (Fig. 4(b)), diblock copolymers A–B form a concentric cylindrical structure with defect in the center of the cylinder, and homopolymers C form an outer cylindrical layer. For $b_1 = 0.1$ (Fig. 5(c)), diblock copolymers A–B form a concentric cylindrical structure in the center of the cylinder, homopolymers C form an outer cylindrical structure, blocks A always aggregate near the interface between copolymers and homopolymers. From Fig. 5, we can see that the domains reverse from the tilted pancakes/cylinder structure ($L_{\perp}^{\rm tilted}$) to the concentric cylindrical structure with holes and to the perfect concentric cylindrical structure ($L_{\parallel}$) with $b_1$ increasing.

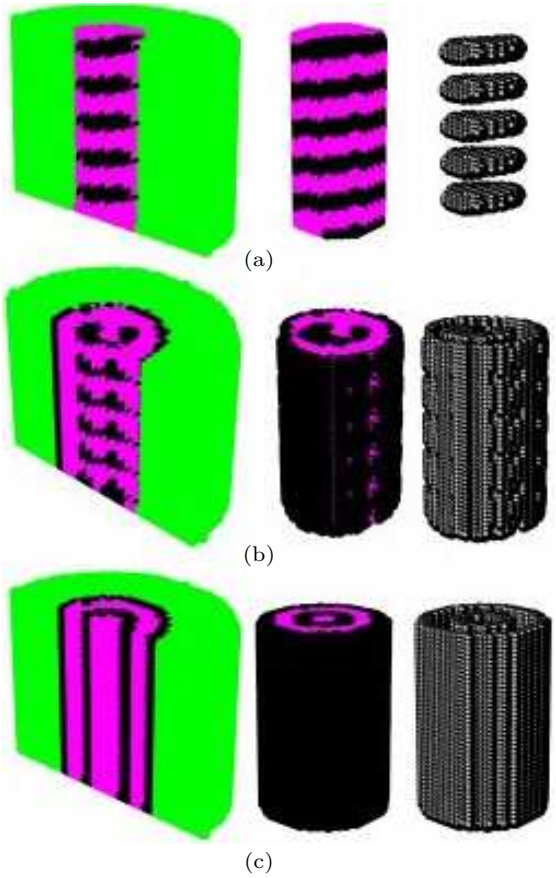



**Fig. 5.** (color online) Morphological patterns constrained within cylinders with varied $b_1$, $L_{\rm pore}/L_0 = 5.63$, (a) $b_1 = 0.001$, (b) $b_1 = 0.035$, (c) $b_1 = 0.1$, the other parameters are the same as those in Fig. 4. The left of each graph shows the section structure, the middle of each graph shows the A–B diblock, the right of each graph shows blocks A. Phase A is represented by the black regions, phase B by the pink regions, phase C by the green regions.

For very small values of $b_1$ (Fig. 5(a)), $\chi_{\rm AC} = 0.227$, $\chi_{\rm BC} = 0.229$, $\chi_{\rm AC} \approx \chi_{\rm BC}$, phases A and B have the same chance to get in touch with phase C. And because the nanopore length and the lamellae spacing are not commensurate, the microphase separated pattern forms a tilted-pancake structure. When $b_1$ increases (Fig. 5(b)), $\chi_{\rm AC} = 0.193$, $\chi_{\rm BC} = 0.263$, the repulsive interaction between the B blocks and homopolymers $(\chi_{\rm BC})$ continues to increase, blocks B gradually leave the macrodomain interface, more A blocks aggregate near the interface, a concentric cylindrical structure with defects appears. When $b_1 = 0.1$ (Fig. 5(c)), $\chi_{\rm AC} = 0.128$, $\chi_{\rm BC} = 0.328$, the repulsive interaction between the B blocks and homopolymers $(\chi_{\rm BC})$ is large enough, it means that the repulsive interaction of the C homopolymers with the B blocks is larger than that with the A block, so it makes the B blocks not favorable in the macrodomain interface, the microphase separated pattern forms a perfect concentric cylindrical structure. According to the result, we can realize the orientational transition by changing the repulsive interaction between monomers, and it can be achieved by selecting different copolymers in experiment.

### 3.5. Effects of the initial composition ratio of copolymer–homopolymer mixtures

In the above research, we find that the C blocks form an outer cylindrical layer in all cases. In order to explain that, we also investigate the effect of the relative concentrations of A–B diblock copolymers and C homopolymers by changing only the initial composition ratio of the A–B copolymers and the C homopolymers. Figure 6 displays the domain pattern at $t = 1000000$ with the composition ratio of C to A–B from 59.4/40.6, 51.4/48.6 to 44.4/55.6, $b_1 = 0.1$, the other parameters are the same as those in Fig. 4, the right side figures in Fig. 6 show the order-parameter profile along $y = 28$, $z = 40$, the red line represents the profile of $\eta$, and the black line is that of $\phi$. From Fig. 6, we can see that blocks A, B, and C form a sequence of concentric cylindrical structures, and the A blocks always aggregate near the interface between copolymers and homopolymers because of the interaction $b_1\eta\phi$. When the composition ratio of C to A–B is 59.4/40.69 (Fig. 6(a)), the diblock copolymers A–B take over the inner cylindrical layer, homopolymers C form the outer cylindrical layer; when the composition ratio is 51.4/48.6 (Fig. 6(b)), the diblock copolymers A–B take over the inner and outer cylindrical layers, homopolymers C form the medial cylindrical layer; when the composition ratio is 44.4/55.6 (Fig. 6(c)), the diblock copolymers A–B take over the outer cylindrical layer, homopolymers C form the inner cylindrical layer.

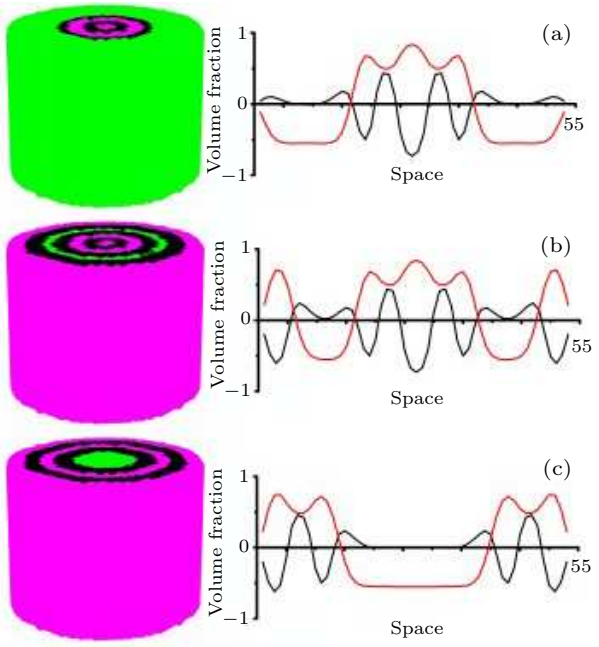



**Fig. 6.** (color online) Morphological patterns constrained within cylinders with various initial composition ratio of C to A–B: (a) 59.4/40.6, (b) 51.4/48.6, (c) 44.4/55.6, $b_1 = 0.1$, the other parameters are the same as those in Fig. 4. The left of each graph shows the three-dimensional structure, the right side figures show the order-parameter profiles, the red line represents the profile of $\eta$, and the black line is that of $\phi$ along $y = 28$, $z = 40$. Phase A is represented by the black regions, phase B by the pink regions, phase C by the green regions.

In the case of $b_1 = 0.1$, the repulsive interaction of the homopolymers with the B blocks is larger than that with the A blocks, so the B blocks are far away from the macrodomain interface, the A blocks appear near the macrodomain interface. On one hand, the free energy minimization consequentially asks for the minimum interface, which makes the macrophase separation come up and the concentric cylindrical structures form. On the other hand, in order to minimize the free energy, there is a tendency for the components of the larger concentration to emerge in the the outer cylindrical layer. The position of the C blocks transforms from the outer cylindrical layer to the medial cylindrical layer and to the inner cylindrical layer with decreasing concentrations of the C blocks.

## 4. Conclusions

In this work, using the CDS approach, we have investigated the self-assembly of copolymer–homopolymer mixtures under cylindrical confinement. We find that much richer morphologies can form in the diblock copolymer–homopolymer mixture in the nanopore than that in the bulk. We propose a minimum two-order-parameter Ginzburg–Landau model. The morphological dependence of nanopore diameter and nanopore length has been systematically studied, the interactions between different monomers and the initial composition ratio of C to A–B are also discussed. The competition of the surface effect and the extension effect results in a series of phase behaviors of the diblock copolymer–homopolymer mixture in neutral nanopores. By changing the interactions between different monomers, we obtain a transition from a tilted pancakes/cylinder structure ($L_{\perp}^{\text{tilted}}$) to a concentric cylindrical structure with defects and to a perfect concentric cylindrical structure ($L_{\parallel}$) with $b_1$ increasing. With the concentration of the C blocks in the mixture decreasing, the position of phase C changes from the outer cylindrical layer to the medial cylindrical layer and then to the inner cylindrical layer. Our model and simulations provide a reference for realizing experimentally ordered structures on the microphase separation consisting of diblock copolymer–homopolymer mixtures and show a possibility for the physical design of soft-matter materials through the adjustment of the size of confined geometries.

## References


[1] Park M, Harrison C, Chainkin P M, Register R A and Adamson D H 1997 *Science* **267** 1401
[2] Li Y Y, Zhou Y and Zhang G Z 2006 *Chin. Phys.* **15** 985
[3] Hamley I W 2003 *Nanotechnology* **14** R39
[4] Park C, Yoon J and Thomas E L 2003 *Polymer* **44** 6725
[5] Wang X H, Li S B, Zhang L X and Liang H J 2011 *Chin. Phys. B* **20** 083601
[6] Broz P, Driamov S, Ziegler J, Ben-Haim N, Marsch S, Meier W and Hunziker P 2006 *Nano Lett.* **6** 2349
[7] Chen W Q, Wei H, Li S L, Feng J, Nie J, Zhang X Z and Zhuo R X 2008 *Polymer* **49** 3965
[8] Sivaniah E, Hayashi Y, Matsubara S, Kiyono S, Hashimoto T, Fukunaga K, Kramer E J and Mates T 2005 *Macromolecules* **38** 1837
[9] Fukunaga K, Hashimoto T, Elbs H and Krausch G 2003 *Macromolecules* **36** 2852
[10] Rong L X, Wei L H, Dong B Z, Hong X G, Li F M and Li Z C 2003 *Chin. Phys.* **12** 771
[11] Olszowka V, Tsarkova L and Boker A 2009 *Soft Matter* **5** 812
[12] Knoll A, Tsarkova L and Krausch G 2007 *Nano Lett.* **7** 843
[13] Zoelen W and Brinke G 2009 *Soft Matter* **5** 1568
[14] Sakurai S 2008 *Polymer* **49** 2781
[15] Xu T, Craig J H and Russell T P 2003 *Macromolecules* **36** 61782
[16] Boker A, Schmidt K, Knoll A, Zettl H, Hansel H, Urban V, Abetz V and Krausch G 2006 *Polymer* **47** 849
[17] Matsen M W 2006 *Soft Matter* **2** 1048
[18] Schmidt K, Boker A, Zettl H, Schubert, Hansel H, Fischer F, Weiss T M, Abetz V, Zvelindovsky A V, Sevink G J A and Krausch G 2005 *Langmuir* **21** 11974
[19] Boker A, Elbs H, Hansel H, Knoll A, Ludwigs S, Zettl H, Zvelindovsky A V, Sevink G J A, Urban V, Abetz V, Muller A H E and Krausch G 2003 *Macromolecules* **36** 8078
[20] Sun M N, Zhang J J, Wang B F, Wu H S and Pan J X 2011 *Phys. Rev. E* **84** 011802
[21] He L L, Zhang R F and Ji Y Y 2012 *Chin. Phys. B* **21** 088301
[22] Pinna M and Zvelindovsky A V 2008 *Soft Matter* **4** 316
[23] Hong Y R, Admson D H, Chainkin P M and Register R A 2009 *Soft Matter* **5** 1687
[24] Kellogg G J, Walton D G, Mayes A M, Lambooy P, Russell T P, Gallagher P D and Satija S K 1996 *Phys. Rev. Lett.* **76** 2503
[25] Huang E, Russell T P, Harrison C, Chaikin P M, Register R A, Hawker C J and Mays J 1998 *Macromolecules* **31** 7641
[26] Han Y Y, Cui J and Jiang W 2008 *Macromolecules* **41** 6239
[27] Wang Q, Yan Q, Nealey P F and de Pablo J J 2000 *Macromolecules* **33** 4512
[28] Matsen M W 1997 *J. Chem. Phys.* **106** 7781
[29] Horvat A, Lyakhova K S, Sevink G J A, Zvelindovsky A V and Magerle R 2004 *J. Chem. Phys.* **120** 1117
[30] Lyakhova K S, Sevink G J A, Zvelindovsky A V, Horvat A and Magerle R 2004 *J. Chem. Phys.* **120** 1127
[31] Horvat A, Sevink G J A, Zvelindovsky A V, Krekhov A and Tsarkova L 2008 *ACS Nano* **2** 1143
[32] Pan J X, Zhang J J, Wang B F, Wu H S and Sun M N 2013 *Chin. Phys. B* **22** 026401
[33] Knoll A, Lyakhova K S, Horvat A, Krausch G, Sevink G J A, Zvelindovsky A V and Magerle R 2004 *Nat. Mater.* **3** 886
[34] Knoll A, Horvat A, Lyakhova K S, Krausch G, Sevink G J A, Zvelindovsky A V and Magerle R 2002 *Phys. Rev. Lett.* **89** 035501
[35] Knoll A, Magerle R and Kraush G 2004 *J. Chem. Phys.* **120** 1105
[36] Xiang H Q, Shin K, Kim T, Moon S I, McCarthy T J and Russell T P 2004 *Macromolecules* **37** 5660
[37] Shin K, Xiang H Q, Moon S I, Kim T, McCarthy T J and Russel T P 2004 *Science* **306** 76
[38] Sun Y, Steinhart M, Zschech D, Adhikari R, Michler G H and Gosele U 2005 *Macromole. Rapid Commun.* **26** 369
[39] Xiang H Q, Shin K, Kim T, Moon S I, McCarthy T J and Russell T P 2005 *Macromolecules* **38** 1055
[40] Xiang H Q, Shin K, Kim T, Moon S I, McCarthy T J and Russell T P 2005 *J. Polym. Sci. Part B: Polym. Phys.* **43** 3377
[41] Dobriyal P, Xiang H Q, Kazuyuki M, Chen J T, Jinnai H and Russell T P 2009 *Macromolecules* **42** 9082
[42] Ma M, Krikorian V, Yu J H, Thomas E L and Rutledge G C 2006 *Nano Lett.* **6** 2969
[43] Ma M, Titievsky K, Thomas E L and Rutledge G C 2009 *Nano Lett.* **9** 1678
[44] Chen D, Zhao W, Wei D G and Russell T P 2011 *Macromolecules* **44** 8020
[45] Wu Y Y, Cheng G S, Katsov K, Sides S W, Wang J F, Tang J, Fredrickson G H, Moskovits M and Stucky G D 2004 *Nat. Mater.* **3** 816
[46] He X H, Song M, Liang H J and Pan C Y 2001 *J. Chem. Phys.* **114** 10510
[47] Sevink G J A, Zvelindovsky A V, Fraaije J G E M and Huinink H P 2001 *J. Chem. Phys.* **115** 8226
[48] Li W H, Wickham R A and Garbary R A 2006 *Macromolecules* **39** 806
[49] Chen P, He X H and Liang H J 2006 *J. Chem. Phys.* **124** 104906
[50] Yu B, Sun P C, Chen T H, Jin Q H, Ding D T, Li B H and Shi A C 2006 *Phys. Rev. Lett.* **96** 138306

[51] Feng J, Liu H L and Hu Y 2006 *Macromol. Theory Simul.* **15** 674
[52] Feng J and Ruckenstein E 2006 *Macromolecules* **39** 4899
[53] Xiao X Q, Huang Y M, Liu H L and Hu Y 2007 *Macromol. Theory Simul.* **16** 732
[54] Sevink G J A and Zvelindovsky A V 2008 *J. Chem. Phys.* **128** 084901
[55] Wang Z, Li B H, Jin Q H, Ding D T and Shi A C 2008 *Macromol. Theory Simul.* **17** 86
[56] Wang Z, Li B H, Jin Q H, Ding D T and Shi A C 2008 *Macromol. Theory Simul.* **17** 301
[57] Pinna M, Guo X H and Zvelindovsky A V 2009 *J. Chem. Phys.* **131** 214902
[58] Chen P, Liang H J and Shi A C 2007 *Macromolecules* **40** 7329
[59] Wang Q 2007 *J. Chem. Phys.* **126** 024903
[60] He X H, Liang H J, Song M and Pan C Y 2002 *Macromol. Theory Simul.* **11** 379
[61] Li W H and Wickham R A 2006 *Macromolecules* **39** 8492
[62] Yu B, Sun P C, Chen T H, Jin Q H, Ding D T, Li B H and Shi A C 2007 *J. Chem. Phys.* **127** 114906
[63] Yu B, Jin Q H, Ding D T, Li B H and Shi A C 2008 *Macromolecules* **41** 4042
[64] Morita H, Kawakatsu T, Doi M, Yamaguchi D, Takenaka M and Hashimoto T 2004 *J. Phys. Soc. Jpn.* **73** 1371
[65] Jiang Y Y, Li H, Li Y F, Yu H Q, Liew K M, He Y Z and Liu X F 2011 *ACS Nano* **5** 2126
[66] Yu H Q, Li H, Zhang J X, Liu X F and Liew K M 2010 *Carbon* **48** 417
[67] Li Y F, Sun F W and Li H 2011 *J. Phys. Chem. C* **115** 18459
[68] Jackson A M, Myerson J W and Stellacci F 2004 *Nat. Mater.* **3** 330
[69] Yabu H, Higuchi T, Ljiro K and Shimomura M 2005 *Chaos* **15** 047505
[70] Yabu H, Higuchi T and Shimomura M 2005 *Adv. Mater.* **17** 2062
[71] Kim H, Daniels E S, Li S, Mokkapati V K and Kardos K 2007 *J. Polym. Sci. Part A: Polym. Chem.* **45** 1038
[72] Such G K, Tjipto E, Postma A, Johnston A P R and Caruso F 2007 *Nano Lett.* **7** 1706
[73] Higuchi T, Yabu H and Shimomura M 2007 *J. Nanosci. Nanotechnol.* **7** 856
[74] Tajima A, Higuchi T, Yabu H and Shimomura M 2007 *Colloids and Surfaces A: Physicochem. Eng. Aspects* **313–314** 332
[75] Rider D A, Chen J I L, Eloi J C, Arsenault A C, Russell T P, Ozin G A and Manners I 2008 *Macromolecules* **41** 2250
[76] Higuchi T, Tajima A, Yabu H and Shimomura M 2008 *Soft Matter* **4** 1302
[77] Tang P, Qiu F, Zhang H D and Yang Y L 2005 *Phys. Rev. E* **72** 016710
[78] Li L, Matsunaga K, Zhu J T, Higuchi T, Yabu H, Shimomura M, Jinnai H, Hayward R C and Russell T P 2010 *Macromolecules* **43** 7807
[79] Pinna M, Hiltl S, Guo X H, Boker A and Zvelindovsky A V 2010 *ACS Nano* **4** 2845
[80] Huh J, Jung J Y, Lee J U, Cho H, Park S, Park C and Jo W H 2011 *ACS Nano* **5** 115
[81] Zhang J J, Jin G J and Ma Y Q 2005 *Phys. Rev. E* **71** 051803
[82] Zhang J J, Jin G J and Ma Y Q 2005 *Eur. Phys. J. E* **18** 359
[83] Zhang J J, Jin G J and Ma Y Q 2006 *J. Phys.: Condens. Matter* **18** 837
[84] Ohta T and Ito A 1995 *Phys. Rev. E* **52** 5250
[85] Ito A 1998 *Phys. Rev. E* **58** 6158
[86] Komura S and Kodama H 1997 *Phys. Rev. E* **55** 1722
[87] Roan J and Shakhnovich E I 1999 *Phys. Rev. E* **59** 2109
[88] Oono Y and Puri S 1987 *Phys. Rev. Lett.* **58** 836
[89] Puri S and Oono Y 1988 *Phys. Rev. A* **38** 1542
[90] Oono Y and Puri S 1988 *Phys. Rev. A* **38** 434
[91] Shinozaki A and Oono Y 1992 *Phys. Rev. A* **45** R2161
[92] Shinozaki A and Oono Y 1993 *Phys. Rev. E* **48** 2622